Journal of
Water & Climate Change



IWA PUBLISHING



Journal of Water and Climate Change Vol 15 No 9, 4278 doi: 10.2166/wcc.2024.012

# Impacts of climate change and variability on drought characteristics and challenges on sorghum productivity in Babile District, Eastern Ethiopia

Abdisa Alemu Tolossa[a,*], Diriba Korecha Dadi[b], Lemma Wogi Mirkena[c], Zelalem Bekeko Erena[c] and Feyera Merga Liben[d]

[a] Haramaya University College of Agricultural and Environmental Sciences, Haramaya, Ethiopia
[b] Famine Early Warning Systems Networks, P.O. Box 5689, Addis Ababa, Ethiopia
[c] Haramaya University, Haramaya, Ethiopia
[d] International Livestock Research Institute (ILRI), P.O. Box 5689, Addis Ababa, Ethiopia
*Corresponding author. E-mail: abdissa.alemu@haramaya.edu.et

AAT, 0000-0002-9318-2530

## ABSTRACT

Examining the characteristics of drought indices in the context of climate variability and change, particularly in semi-arid water-stressed regions, requires adaptation. Observed climate data of the Babile station from 1980 to 2009 were used as a baseline for climate projection. Future climate projection was established under two Representative Concentration Pathway (RCP4.5 and RCP8.5) climate scenarios for the 21st century. Two drought indices, namely standard precipitation index and standard evapotranspiration index (SPI and SPEI) were employed based on temperature and rainfall to characterize droughts. Our study revealed that drought severity and intensity are more likely to increase under RCP4.5 climate forcing in the middle of the 21st century. The average drought severity (S) was 1.1, 1.53, 1.55, and 1.8 in SPEI 3-month time scale; 1.51, 2.1, 2.38, and 2.29 in SPEI 4-month time scale; and 2.15, 2.77, 3.44, and 2.91 in SPEI 6-month time scale, whereas, the drought severity (S) was 1.33, 1.37, and 1.79 in SPEI 3-month time scale; 1.79, 2.05, and 2.19 in SPEI 4-month time scale; and 2.47, 3.19, and 2.69 in SPEI 6-month time scale in observed, near, mid and end of the 21st century under RCP4.5 and 8.5 scenarios, respectively. Increase in drought frequency and severity occurrences under RCP4.5 scenario would have a negative impact on sorghum crop productivity. We recommended further study on practical soil water conservation to drought management in the study area.

**Key words:** climate change, climate projection, drought characteristics, drought indices

## HIGHLIGHTS

- Drought duration, severity, and intensity will increase in future mainly under the RCP4.5 scenario.
- Temperature increases under both RCP4.5 and RCP8.5 scenarios but rainfall has mixed signals under different climate scenarios.
- SPEI trend decreases in the 21st century from observation time to end-century.

## GRAPHICAL ABSTRACT

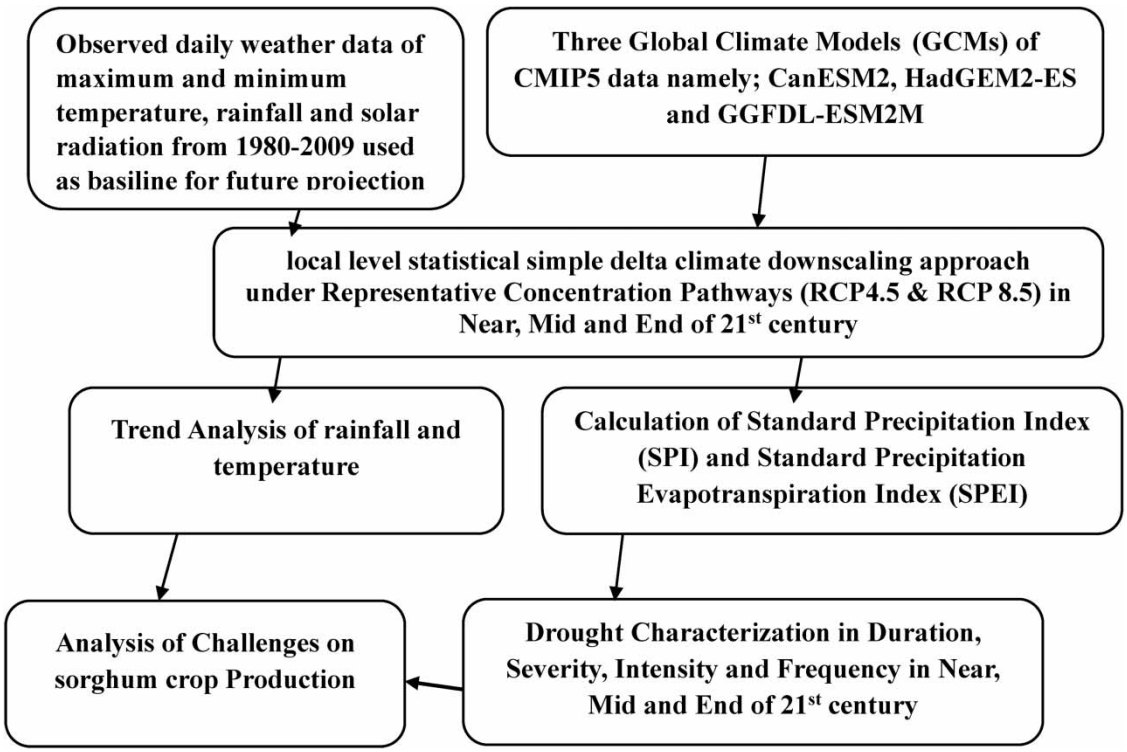


## 1. INTRODUCTION

Drought is a complex phenomenon, and it originates from a deficiency of rainfall relative to long-term average that extends over a given space and time scale for a specific period, leading to soil water shortage (Mishra & Singh 2010; Van Loon 2015), while others scholars defined drought based on the period of abnormal arid conditions (Eslamian *et al.* 2017). Based on different scholars, the most common drought would be classified into four types including meteorological (precipitation), agricultural (soil moisture), hydrological, and socioeconomic droughts (Mishra & Singh 2010). Since the 1990s, the frequency and intensity of drought events have been increasing globally under the combined effects of changing climate, environmental conditions, and human activities (Omer *et al.* 2020). However, sorghum is drought tolerant compared to other cereal crops and can cope with different types of stresses (Ejeta & Knoll 2007). The occurrence of post-flowering drought often causes premature plant death, lodging, reduction in seed size and ultimately grain yield losses, its production is significantly influenced by climate change and variability (Srivastava *et al.* 2010).

Assessment of the impacts of climate change on drought characteristics at the local level and their future projections by using global circulation models (GCMs) is important for adaption planning (Endris *et al.* 2013; Ahmed *et al.* 2018). Thus, several studies have used GCMs for the projection of future climate change impact evaluation under different climate scenarios (Zhou *et al.* 2016). The impact of climate change on drought characteristics reported based on five GCMs in the Coupled Model Inter-comparison Project (CMIP5) showed a decline in rainfall amount in East Africa in the 21st century that led to an increase in drought intensity and frequency over most of East Africa like Ethiopia (Haile *et al.* 2020). Even though drought is a complex phenomenon, many drought indices such as Standard Precipitation Evapotranspiration Index (SPEI) and Standard Precipitation Index (SPI) have been used for quantifying and monitoring drought characterization (Vicente-Serrano *et al.* 2010; Wang *et al.* 2019). Drought characteristics by SPEI that included the potential evapotranspiration (PET) method are preferable indices suited for studies of the effect of global warming on drought severity and is more preferable to monitor and evaluate water balance conditions and also performed well in measuring droughts characteristics (Vicente-Serrano *et al.* 2010; Wang *et al.* 2019).

Our present study evaluates the state of frequency and intensity of drought indices by using SPI and SPEI methods in semi-arid parts of East Hararghe Zone Babile district, where drought frequently affects crop production. Based on the rainfall anomaly index, the severe droughts that occurred in the Babile district during crop production season (JJAS) were 1987, 1991, 2000, 2002, 2005, 2010, 2011, and 2015 among which 2002 and 2010 were the severe drought intensity in recent history (Tolosa *et al.* 2023). Here, there is a limited study of future climate change impact on drought character interactive impact on the crop productivity in the study area. However, few studies have been conducted in Ethiopia under current and future climate change scenarios over high spatial dimension (Teshome & Zhang 2019). The present study therefore aimed to analyze the impacts of climate change in drought characteristics at local level and its challenges on sorghum crop productivity in the Babile District semi-arid region of East Hararghe Zone, Ethiopia.

## 2. MATERIALS AND METHODS

### 2.1. Description of the study area

The study was conducted in the Babile District, East Hararghe Zone, which is located in Oromia Regional National State, eastern Ethiopia. The Babile District is located between 8.35°N to 9.18°N, and 42.25°E to 42.9°E, an altitude range of 950–2,000 above sea level and most of the land is under arid and semi-arid climate type (MoA 1998). The physical distance of Babile District from Addis Ababa is 560 km to the east, while it is 35 km from Harar City to the east (Figure 1). The rainfall patterns of East Hararghe Zone are bimodal type, with two rainy seasons, March to May (*Belg*) and June to September (*Kiremt*) are highly erratic, with a long dry season October to February (Bega) (NMSA 1996). According to NMSA, (1996) agro-climate classification, the Babile District is classified under semi-arid areas with a length of growing period between 75 and 120 days. The average annual rainfall of the district is 731 mm, while the average rainfall during the March to May (MAM) and June to September (JJAS) seasons was 301 and 334.6 mm, respectively (Tolosa *et al.* 2023).

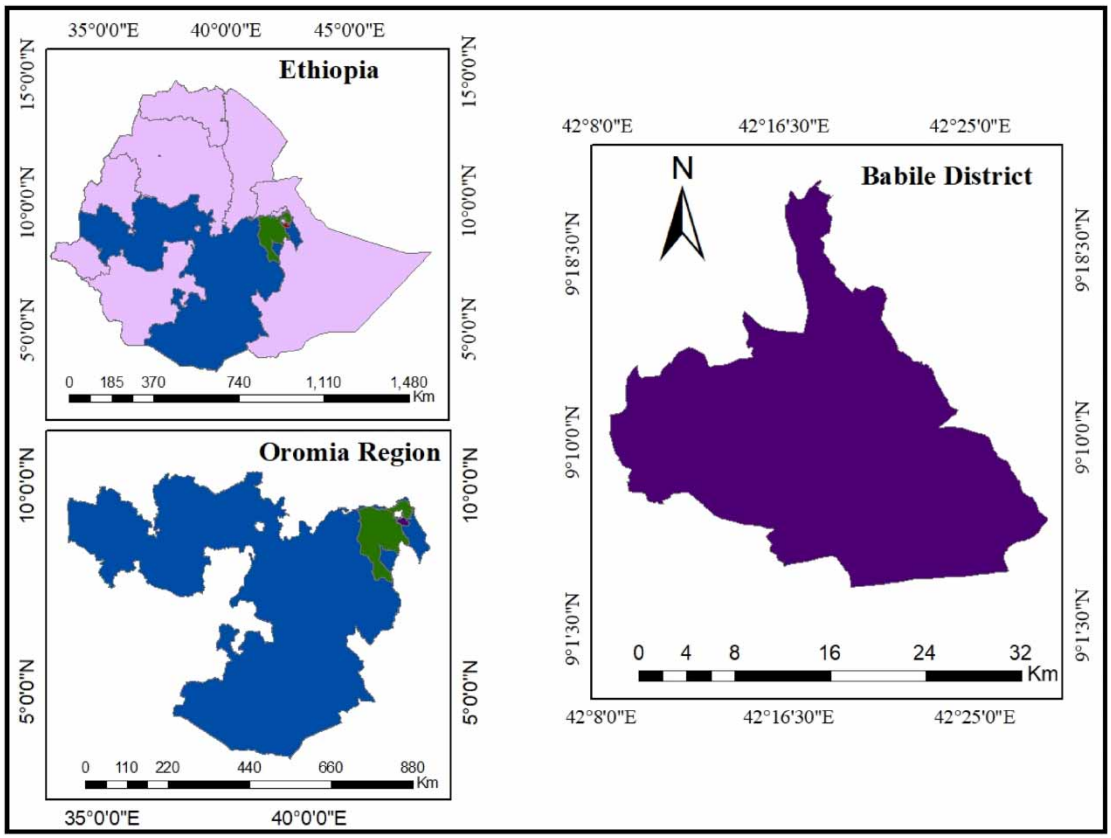


**Figure 1** | Map of the study area.

### 2.2. Sources and types of data

In this study, daily rainfall, and maximum and minimum air temperature data recorded at Babile meteorological station from 1980 to 2009 were used as a baseline for future projection. Continuous and completed daily incident solar radiation were obtained from the NASA website (http://power.larc.nasa.gov/). Global climate model (GCMs) data of CMIP5 was downloaded from the Agricultural Model inter-comparison and Improvement Project (AgMIP) website (https://github.com/agmip/Climate-ScenariosGenerator/tree/master/data/).

### 2.3. Statistical downscaling for future climate projection

Historical and future climate simulations of the 20th and 21st centuries produced by the International Protocol of Climate Change (IPCC) Assessment Report 5 (AR5) participating models and analyzed through the Climate Model Inter-comparison Project Phase 5 (CMIP5) initiative were used in the present study as documented by Taylor *et al.* (2012). The analysis of climate projections is based on moderate Representative Concentration Pathways (RCP 4.5) and high forcing (RCP 8.5) emission scenarios. To make projections for climate change scenarios at the station level, downscaling was performed with historical daily weather data at Babile station of the study area using a simple delta approach technique employed by three global climate models (GCMs) namely; Canadian Earth System Model second generation (CanESM2), Hadley Centre Global Model Earth System (HadGEM2-ES) and Geophysical Fluid Dynamics Laboratory Earth System Model version 2M (GGFDL-ESM2M) under RCP4.5 and RCP8.5 climate change scenarios. The three GCMs Climate Models were selected based on their better performance in resolution and simulation of both historical and long-term climate normal (Chylek *et al.* 2011; Martin & Bellouin 2011; Dunne *et al.* 2013).

Scientific descriptions of the GCMs were well documented in various literatures; HadGEM2 (from UK Met Office Hadley Centre has a spatial resolution of $1.2° \times 1.8°$ (Martin & Bellouin 2011); CanESM2 from Canadian Centre for Climate Modeling spatial resolution of $2.8° \times 2.8°$ (Chylek *et al.* 2011); GFDL-ESM2M from National Oceanic and Atmospheric Administration, USA with spatial resolution of $2.02° \times 2.50°$ (Dunne *et al.* 2013). Because of having lower spatial resolution of the GCMs result output, GCMs data cannot be used directly for local climate change impact assessment (Sunyer *et al.* 2012). Thus, GCMs at large spatial scales are translated to scales more representative of local environmental conditions using downscaled techniques based on Ekstrom *et al.* (2015). Here, future climate projections were created based on baseline climate data from 1980 to 2009 by utilizing the Agricultural Model Inter-comparison and Improvement Project (AgMIP) method of CMIP5 data using a simple 'delta' statistical downscaled approach at the station-level using R software version 4.2 for the period of 2010–2039 (near), 2040–2069 (mid) and 2070–2100 end of the 21st century under RCP4.5 and RCP 8.5 climate scenarios. Besides, the ensemble means across GCM of the future downscaled climate data output were used based on Wallach *et al.* (2016) for future drought characterization.

### 2.4. Analysis of average and trend of rainfall and temperature under different scenarios

The monthly average rainfall and temperature in the baseline (1980–2009), near (2010–2039), mid (2040–2069) and end 2070–2100 of the 21st century were computed under RCP4.5 and RCP8.5 climate scenarios. Monthly trends of statistical tests of rainfall and temperature were computed by R software using the Trend package based on Pohlert (2016).

### 2.5. Drought evaluation using the SPI

The SPI is used to characterize drought and is designed to quantify precipitation deficit for multiple time scales by a probability distribution based on McKee *et al.* (1993). Here, SPI-3, SPI-4 and SPI-6-month time scales were calculated by fitting a gamma distribution that has been found to fit the monthly rainfall deficit series using the R software version 4.2 in the SPEI package tool. The gamma probability density function was first fitted to a given frequency distribution of precipitation as follows:

$$g(x) = \frac{1}{\beta^{\alpha}\gamma(\alpha)} X^{\alpha-1} e^{\frac{X}{\beta}} \tag{1}$$

where $g(x)$ is the probability distribution function, $x$ is the rainfall amount ($x > 0$), $\gamma(\alpha)$ is the gamma function as defined by Thom (1966), $\alpha$ and $\beta$ are shape ($\alpha > 0$) and scale ($\beta > 0$) parameters determined by the maximum likelihood method

(Thom 1966) based on Equations (2)–(5):

$$\gamma(\alpha) = \int_0^\infty y^{\alpha-1} e^{-y} dy \tag{2}$$

$$\alpha = \frac{1}{4u}\left(1 + \sqrt{1 + \frac{4u}{3}}\right) \tag{3}$$

$$u = \ln(\bar{X}) - \frac{\sum \ln(X)}{n} \tag{4}$$

$$\beta = \frac{\bar{X}}{\alpha} \tag{5}$$

where '$n$' is the number of observations, then the cumulative probability function is given by (Thom 1966) as shown in Equations (6) and (7):

$$G(x) = \int_0^x g(x) dx \tag{6}$$

The cumulative probability was modified by Thom (1966):

$$G_m(x) = p + (1-p)G(x) \tag{7}$$

where '$p$' is the probability of no rainfall at a specified time scale, the cumulative probability distribution $G_m(x)$ is then transformed into a standardized normal distribution of the SPI with the average equal to 0 and standard deviation being 1 as documented by Zelen & Severo (1965) based on Equations (8)–(11):

$$\text{SPI} = -\left(t - \frac{co + c1t + c2t^2}{1 + d1t + d2t^2 + d3t^3}\right) \quad \text{For } 0 < G_m(x) \leq 0.5 \tag{8}$$

$$\text{where} \quad t = \sqrt{\ln\left(\frac{1}{(G_m(x))2}\right)} \quad \text{For } 0 < G_m(x) \leq 0.5 \tag{9}$$

$$\text{SPI} = +\left(t - \frac{c0 + c1t + c2t^2}{1 + d1t + d2t^2 + d3t^3}\right) \quad \text{For } 0.5 < G_m(x) \leq 1.0 \tag{10}$$

$$\text{where} \quad t = \sqrt{\ln\left(\frac{1}{1 - G_m(x))2}\right)} \quad \text{For } 0.5 < G_m(x) \leq 1.0 \tag{11}$$

$c$ and $d$ are the constants and $c_0 = 2.515517$, $c_1 = 0.802853$, $c_2 = 0.010328$, $d_1 = 1.432788$, $d_2 = 0.189269$ and $d_3 = 0.001308$.

### 2.6. The SPEI

The SPEI with 3-, 4- and 6-month time scales were calculated by fitting a logistic distribution that has been found to fit the monthly water balance data based on Vicente-Serrano *et al.* (2010), using the R software version 4.2 in the SPEI package tool. The SPEI uses 'climatic water balance', the difference between precipitation and reference evapotranspiration ($P - \text{ET}_0$). The use of a particular equation for the estimation of $\text{ET}_0$ is not central to the calculation of the SPEI. Thus, most of the studies have used the Penman–Monteith (PM) equation for the calculation of $\text{ET}_0$ (Allen *et al.* 1998). However, the PM equation requires extensive data (solar radiation, temperature, wind speed, sunshine hour and relative humidity). However, the meteorological station we utilized in this study does not routinely record all of these variables. To solve such a problem, Droogers & Allen (2002) estimate $\text{ET}_0$ by using the Hargreaves (Hg) method. This method was tested in the east-southern area and results showed satisfactory agreement with $\text{ET}_0$–PM estimates (Droogers & Allen 2002).

Drought analysis by the SPEI calculation is subject to the accumulating deficit or surplus ($D_i$) of water balance at different time scales. '$D_i$' can be determined based on precipitation (P) and PET for a given month '$i$'. Here, based on monthly water balance calculations using Equation (12):

$$\text{Water balance}(D_i) = P - \text{ET}_\text{o} \tag{12}$$

Then, the Hargreaves & Samani (1985) method was used to estimate monthly PET employed to calculate reference obtained by the following equation:

$$ET_\text{o} = 0.0135 * kRs * Ra(\sqrt{T_\text{max} - T_\text{min}})\ \ (T_a + 17.8) \tag{13}$$

where 0.0135 is a factor for conversion from American to the international system of units, $kRs$ is the radiation adjustment coefficient (the common value $kRs = 0.17$), $Ra$ is solar radiation at a given latitude, while $T_\text{max}$, $T_\text{min}$ and $T_\text{a}$ are maximum, minimum and average temperature, respectively.

After climatic water balance was calculated at a monthly time scale, the resulting values were fitted to a log-logistic probability distribution to transform the original values to standardized units that are comparable in space and time and at different SPEI time scales based on Vicente-Serrano *et al.* (2010). Here, the probability distribution function of a variable of the water balance ($D_i$) is described according to a logistic distribution as given by the following equation:

$$\text{F(D)} = \left[1 + \left(\frac{\alpha}{D - \gamma}\right)^{\beta}\right]^{-1} \tag{14}$$

where $\alpha$, $\beta$ and $\gamma$ represent the scale, shape and location parameters that are estimated from sample D (difference between precipitation and reference evapotranspiration for a given month), when the log-logistic $\alpha$, $\beta$ and $\gamma$ distribution parameters were calculated, the probability-weighted moments (PWMs) method was used, based on Hosking (1990), and calculated by Equation (15) as follows:

$$PWMs = \frac{1}{N}\sum_{i=1}^{N}(1 - F_i)^S D_i \tag{15}$$

where '$N$' is the number of data, '$F_i$' is a frequency estimator following the approach of Hosking (1990) and '$D_i$' is the difference between precipitation and potential evapotranspiration for the month '$i$'. The function of the SPEI with different time scale is computed by Equation (16):

$$\text{SPEI} = W - \frac{C_{o+C_1W+C_2W^2}}{1 + d_1W + d_2W^2 + d_3W^3} \tag{16}$$

When $P \leq 0.5$, $W = \sqrt{-2\ln(P)}$, and when $P > 0.5$, $W = \sqrt{-2\ln(1-P)}$, $C_o = 2.5155$, $C_1 = 0.8028$, $C_2 = 0.0203$, $d_1 = 1.4327$, $d_2 = 0.1892$, $d_3 = 0.0013$.

### 2.7. Analysis of drought duration, intensity, and severity

The drought characteristics in terms of frequency, duration, severity, and intensity were calculated at the local level based on Adhyani *et al.* (2017). Here, the drought duration ($D$) is the period length in which the SPEI is continuously negative, starting from the SPEI values equal to −1 and ending when the SPEI values turn out to be positive values as indicated in Figure 2. The drought severity (S) is the cumulated SPEI value within the drought duration, which is defined by a drought event considered when the values of the SPEI fall below zero, a period with negative SPEI values (Figure 2), while the drought intensity (I) is the ratio of the severity of drought to its duration. Currently, drought duration and severity were done based on a run theory

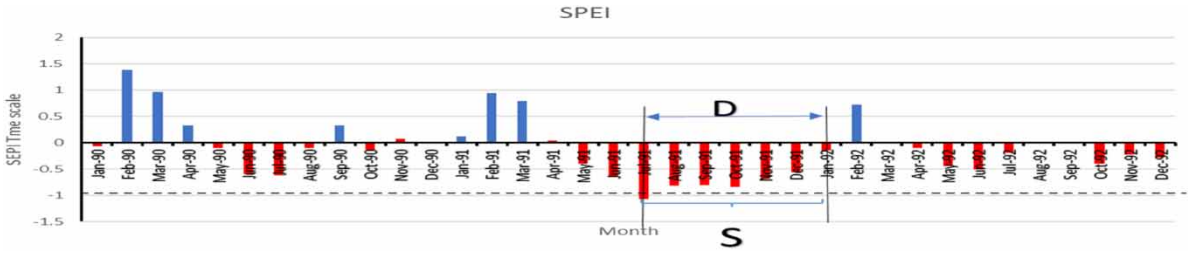


**Figure 2** | Definition of drought characteristics.

using the drought package in R software version 4.2 as follows:

$$S = -\sum_{i=1}^{D} \mathrm{SPEI}_i \text{ and } I = \frac{S}{D}\ F = \frac{n}{N} * 100\% \tag{17}$$

where drought frequency is defined as the number of months in a 30-year period having a value of drought events (SPEI $< -1.0$), $n$ is the number of drought events, and $N$ is the total number of months.

## 3. RESULTS AND DISCUSSION

### 3.1. Temporal change of monthly average rainfall and temperature

The average temperature and rainfall of ensemble means of downscaled climate data across the three GCMs over 30-year time periods as a baseline (1980–2009), near term (2010–2039), mid-term (2040–2069) and end of the 21st century (2070–2100) shown in Figure 3. Looking at average values provides the magnitude of monthly average temperature which will be 32 and 36 ºC at the end of the 21st century under RCP4.5 and RCP8.5 respectively (Figure 3). While the average monthly rainfall most likely during March to May (MAM) will be 160 and 240 mm under RCP4.5 and RCP8.5 respectively (Figure 3).

### 3.2. Analysis of rainfall and temperature trend in ensemble mean across GCMs

In ensemble means across the GCMs model output shows rainfall during October to December (OND) and July are projected to increase, while rainfall in September shows a decreasing trend under the RCP4.5 scenario (Table 1). Similarly, the rainfall amount in OND, MAM, and annual total rainfall as well as monthly rainfall amount in April, July and November showed a statistically significant increasing trend ($P < 0.05$) under the RCP8.5 climate scenario (Table 2). However, the rainfall trend is not significant during the sorghum growing period from June to September, its amount shows a mixed signal of decreasing and increasing under RCP 4.5 and RCP8.5 climate scenarios, respectively (Tables 1 and 2). The annual maximum temperature

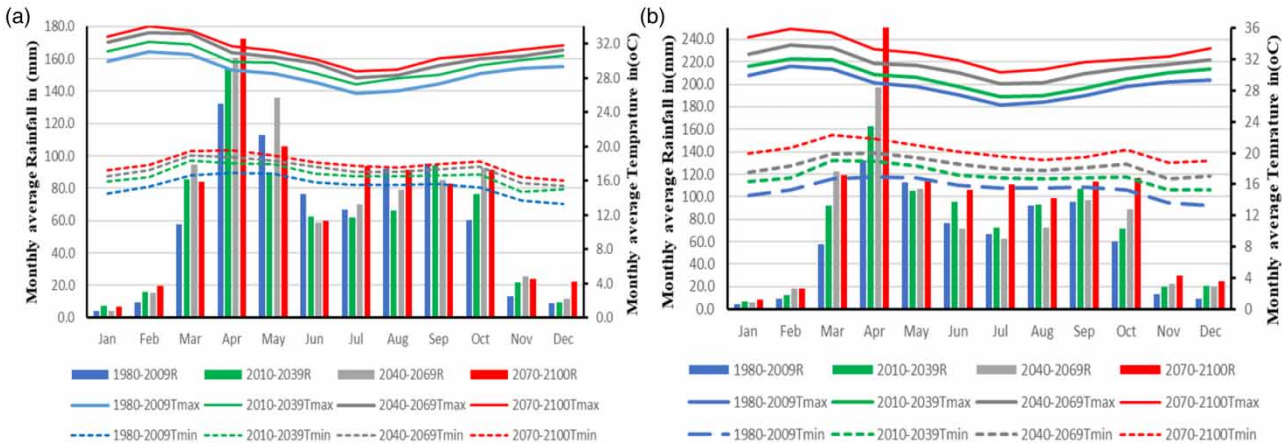


**Figure 3** | Monthly average rainfall and temperature under different periods and scenarios.

**Table 1** | Analysis of rainfall and temperature trend under the RCP4.5 scenario at the Babile station

| | Ensemble mean GCM rainfall (1980–2100) | | | Ensemble mean GCM of maximum *T* (1980–2100) | | | Ensemble mean GCM of minimum *T* (1980–2100) | | |
|---|---|---|---|---|---|---|---|---|---|
| **Time series** | **MKST** | **Sen's slope** | ***P* value** | **MKST** | **Sen's slope** | ***P* value** | **MKST** | **Sen's slope** | ***P* value** |
| Jan | 0.545 | 0.00 | 0.585 | 9.158 | 0.03*** | 0.000 | 3.81 | 0.022*** | 0.000 |
| Feb | 0.425 | 0.00 | 0.670 | 7.95 | 0.039*** | 0.000 | 3.92 | 0.022*** | 0.000 |
| Mar | 0.831 | 0.043 | 0.405 | 6.75 | 0.038*** | 0.000 | 5.11 | 0.026*** | 0.000 |
| April | 0.707 | 0.117 | 0.479 | 6.46 | 0.034*** | 0.000 | 8.06 | 0.027*** | 0.000 |
| May | 0.409 | 0.080 | 0.681 | 6.16 | 0.033*** | 0.000 | 7.92 | 0.022*** | 0.000 |
| June | −1.458 | −0.138 | 0.144 | 6.42 | 0.031*** | 0.000 | 8.11 | 0.022*** | 0.000 |
| July | 2.27 | 0.281* | 0.0227 | 6.826 | 0.027*** | 0.000 | 7.59 | 0.021*** | 0.000 |
| Aug | −0.324 | −0.033 | 0.745 | 6.70 | 0.024*** | 0.000 | 8.47 | 0.021*** | 0.000 |
| Sept | −2.285 | −0.213* | 0.022 | 8.047 | 0.035*** | 0.000 | 9.32 | 0.026*** | 0.000 |
| Oct | 1.138 | 0.114 | 0.25 | 6.066 | 0.027*** | 0.000 | 6.55 | 0.029*** | 0.000 |
| Nov | 1.737 | 0.012 | 0.082 | 6.172 | 0.023*** | 0.000 | 5.99 | 0.027*** | 0.000 |
| Dec | 0.855 | 0.00 | 0.39 | 7.70 | 0.026*** | 0.000 | 4.26 | 0.023*** | 0.000 |
| OND | 2.179 | 0.336* | 0.029 | 7.64 | 0.025*** | 0.000 | 5.71 | 0.026*** | 0.000 |
| MAM | 0.907 | 0.333 | 0.36 | 7.596 | 0.036*** | 0.000 | 7.51 | 0.024*** | 0.000 |
| JJAS | −0.486 | −0.179 | 0.626 | 8.573 | 0.029*** | 0.000 | 9.27 | 0.023*** | 0.000 |
| Annu | 1.26 | 0.76 | 0.205 | 10.58 | 0.031*** | 0.000 | 7.33 | 0.022*** | 0.000 |

Note: Mann–Kendall Statistical Test (MKST) and T = Temperature while * and *** The trend at the significance level of $p = 0.05$ and $p < 0.01$ respectively.

**Table 2** | Analysis of rainfall and temperature trend under the RCP8.5 scenario at the Babile station

| | Ensemble mean GCM of rainfall (1980–2100) | | | Ensemble mean GCM of maximum *T* (1980–2100) | | | Ensemble mean GCM of minimum *T* (1980–2100) | | |
|---|---|---|---|---|---|---|---|---|---|
| **Time series** | **MKST** | **Sen's slope** | ***P* value** | **MKST** | **Sen's slope** | ***P* value** | **MKST** | **Sen's slope** | ***P* value** |
| Jan | 0.958 | 0.00 | 0.338 | 11.46 | 0.055*** | 0.000 | 6.16 | 0.050*** | 0.000 |
| Feb | 0.399 | 0.00 | 0.689 | 10.01 | 0.059*** | 0.000 | 6.84 | 0.05*** | 0.000 |
| Mar | 1.80 | 0.201 | 0.072 | 8.918 | 0.055*** | 0.000 | 8.01 | 0.054*** | 0.000 |
| April | 2.354 | 0.6834* | 0.0185 | 8.448 | 0.051*** | 0.000 | 10.36 | 0.051*** | 0.000 |
| May | 0.387 | 0.0476 | 0.698 | 8.573 | 0.051*** | 0.000 | 10.56 | 0.043*** | 0.000 |
| June | 0.734 | 0.0962 | 0.46 | 8.69 | 0.050*** | 0.000 | 10.08 | 0.043*** | 0.000 |
| July | 2.459 | 0.345* | 0.013 | 9.20 | 0.046*** | 0.000 | 9.73 | 0.041*** | 0.000 |
| Aug | −0.862 | −0.095 | 0.388 | 9.53 | 0.045*** | 0.000 | 11.07 | 0.039*** | 0.000 |
| Sept | −0.15 | −0.023 | 0.88 | 9.876 | 0.050*** | 0.000 | 11.5 | 0.043*** | 0.000 |
| Oct | 1.575 | 0.207 | 0.115 | 8.34 | 0.041*** | 0.000 | 8.98 | 0.053*** | 0.000 |
| Nov | 2.09* | 0.031* | 0.036 | 8.226 | 0.035*** | 0.000 | 8.42 | 0.051*** | 0.000 |
| Dec | 0.831 | 0.00 | 0.405 | 9.875 | 0.043*** | 0.000 | 7.93 | 0.057*** | 0.000 |
| OND | 2.79 | 0.502** | 0.0052 | 9.70 | 0.039*** | 0.000 | 8.75 | 0.053*** | 0.000 |
| MAM | 2.68 | 1.260** | 0.0073 | 9.89 | 0.053*** | 0.000 | 10.27 | 0.049*** | 0.000 |
| JJAS | 0.849 | 0.352 | 0.395 | 10.54 | 0.047*** | 0.000 | 11.36 | 0.042*** | 0.000 |
| Annu | 3.34 | 2.911*** | 0.0008 | 12.56 | 0.048*** | 0.000 | 9.84 | 0.046*** | 0.000 |

*Note:* MKST, Mann–Kendall Statistical Test; *T*, temperature.

*, **, and *** indicate the trend at the significance level of $p = 0.05$, $p = 0.01$, and $p < 0.01$, respectively.

showed an increase of 0.31 °C every 10 years and the annual minimum temperature increased by 0.22 °C every 10 years under the RCP4.5 scenario (Table 1), whereas the annual maximum and minimum temperature increases by 0.48 and 0.46 °C every 10 years under the RCP8.5 scenario (Table 2).

The rising temperatures also increase soil evaporation (Abtew & Melesse 2013), and diminish soil moisture availability (Grillakis 2019; Ogunrinde *et al.* 2022). Thus, the decline in rainfall and an incline in both maximum and minimum temperatures lead mainly to higher moisture stress and reduced crop yield (Singh *et al.* 2017; Gong *et al.* 2021). However, sorghum is the most drought resistant crop (Ejeta & Knoll 2007). Further support in the selection of moisture-stressed resistance sorghum varieties, more soil moisture conservation practices and crop management would be promoted by developing climate resilient varieties as suggested by FAO (2010) in the mid and end of the 21st century mainly under the RCP4.5 climate scenario.

### 3.3. Drought characteristics in the SPI and SPEI

The rainfall trend varies in monthly and seasonal time scale, but temperature trend increases towards the 21st century under both RCP4.5 and RCP8.5 climate scenarios. Consequently, the drought intensity and severity increase towards the the 21st century mainly under RCP 4.5 climate scenario. The result revealed that the SPEI 3-month, 4-month, and 6-month time scales have greater positive oscillations under RCP8.5 than RCP4.5 climate scenarios, especially toward the end of the 21st century than the SPI (Figure 4). The SPEI results showed good agreement with other related studies that global warming may increase the severity and frequency of drought in the future (Ogilvie *et al.* 2013). This is because the SPI is not able to capture drought induced by elevated temperature or evaporative demand (Vicente-Serrano *et al.* 2010; Meresa *et al.* 2016). The SPEI results showed good agreement with other related studies that global warming may increase the severity and frequency of drought in the future (Ogilvie *et al.* 2013).

### 3.4. Drought characteristics and its categories

The results further revealed drought characteristics such as duration, severity and intensity in SPEI 3-, SPEI 4-, and SPEI 6-month time scales under RCP4.5 and RCP8.5 climate scenarios. According to this pattern of drought indices from 1980 to 2100, Babile station experienced an increasing trend in the frequency and severity of droughts mainly under RCP4.5 climate forcing. The drought events in SPEI-3-month scale were 15, 16, 20 and 22 during observed, near, mid and end of the 21st century under RCP4.5 scenario (Table 3). Similarly, drought events in SPEI-4-month scale result were 13, 13, 14 and 18 during observed, near, mid and end of 21st century, respectively under RCP4.5 scenario (Table 4). Besides, in the SPEI-6-month also show 11, 11, 10 and 14 drought events (Table 5) under RCP4.5 scenario at the Babile District. Similarly, drought events in the SPEI-3-month scale were 14, 25, and 22 during near, mid and end of the 21st century (Table 3) and drought events in SPEI-4-month scale result were 12, 18 and 18 during near, mid and end of 21st century (Table 4), while drought events in the SPEI-6-month scale were 10, 12 and 14 drought events (Table 5) under RCP8.5 scenario at the Babile District.

The average drought durations (*D*) were 2.8, 3.5, 3.6, and 3.7 months in SPEI 3-month (Table 3), 3.85, 4.54, 4.71, and 4.33 months in SPEI 4-month (Table 4) and 4.64, 5.64, 6.2 and 5 months in SPEI 6-month under RCP4.5 during observed, near, mid and end of 21st century, respectively (Table 5). Similarly, the average drought durations (*D*) were 3.21, 3.2, and 3.37 months in SPEI 3-month (Table 3), 4.17, 4, and 4.1 months in SPEI 4-month (Table 4) and 5, 6.7, and 4.8 months in SPEI 6-month (Table 5) under RCP8.5 during near, mid, and end of 21st century. The average drought severity (S) was 1.1, 1.53, 1.55, and 1.8 in SPEI 3-month (Table 1) and 1.51, 2.1, 2.38, and 2.29 in SPEI 4-month (Table 4) and 2.15, 2.77, 3.44, and 2.91 in SPEI 6-month under the RCP4.5 scenario during observed, near, mid and end of 21st century (Table 5), whereas, the drought severity (S) was 1.33, 1.37, and 1.79 in SPEI 3-month (Table 3), 1.79, 2.05 and 2.19 in SPEI 4-month (Table 4) and 2.47, 3.19, and 2.69 in SPEI 6-month (Table 5) in near, mid and end of the 21st century under the RCP8.5 scenario.

The overall intensities of SPEI 3-month drought intensity (I) were 0.25, 0.31, 0.36 and 0.36 during the observed, near, mid and end of 21st century (Table 3) under the RCP4.5 scenario. The overall intensities of SPEI 4-month were 0.25, 0.31, 0.36, and 0.38 (Table 4) and SPEI 6-month were 0.29, 0.3, 0.4, and 0.39 (Table 5) during observed, near, mid and end of 21st century under the RCP4.5 scenario. The SPEI 3-month drought intensity (I) was 0.28, 0.249 and 0.401 during the near, mid and end of the 21st century (Table 3) under the RCP8.5 scenario. SPEI 4-month drought intensity was 0.262, 0.343, and 0.374 (Table 4) and SPEI 6-month were 0.308, 0.35, and 0.332 (Table 5) during the near, mid and end of the 21st century under the RCP8.5 scenario. Here, the drought duration, severity and intensity would be increased toward the 21st

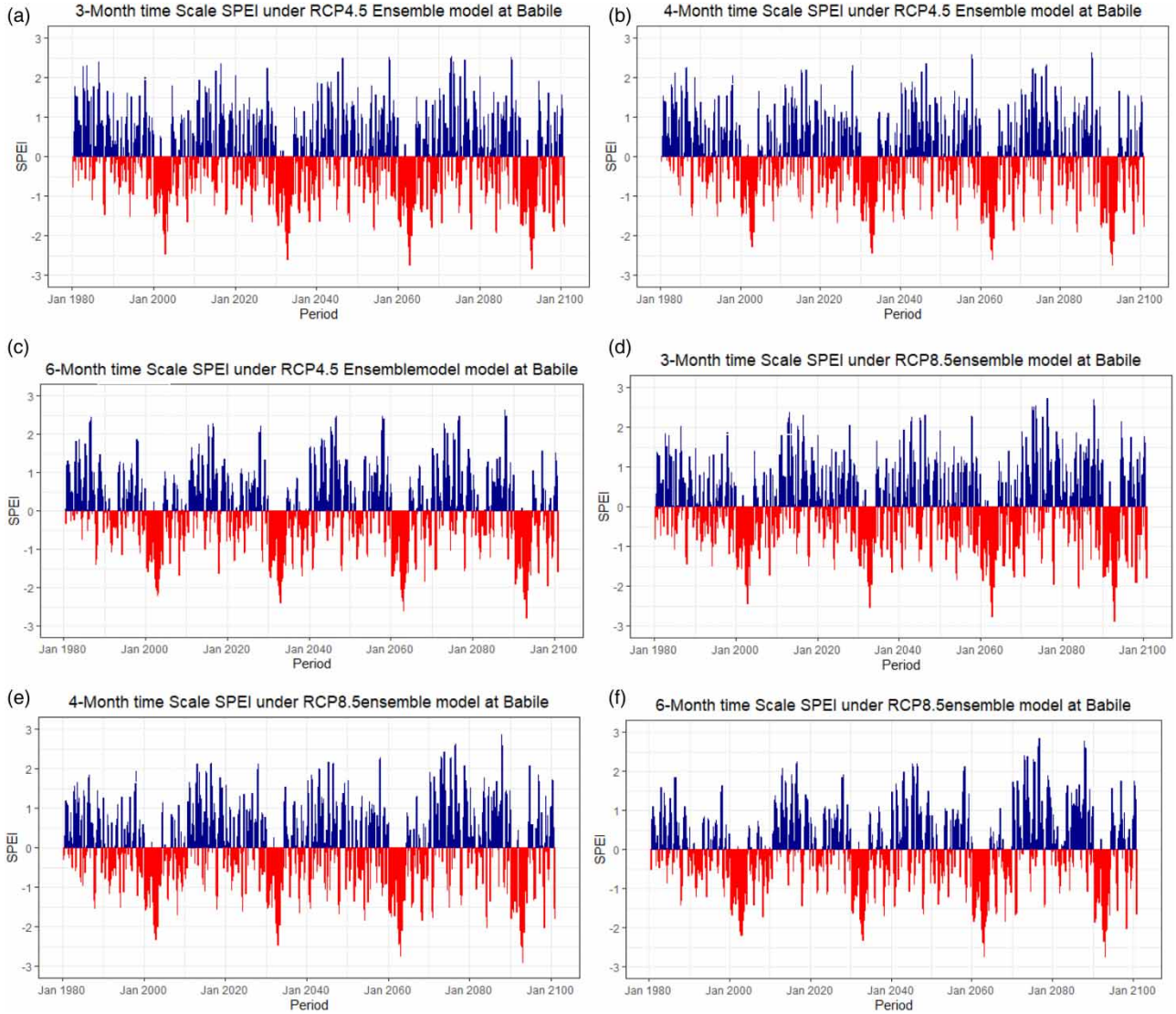


**Figure 4** | SPEI indices in ensemble models under RCP4.5 and 8.5 scenarios.

**Table 3** | Drought characteristics in SPEI-3 based on ensemble mean across three GCMs

| | Under RCP4.5 climate forcing | | | | | Under RCP8.5 climate forcing | | | | |
|---|---|---|---|---|---|---|---|---|---|---|
| **Period** | **Time** | **D** | **LongD** | **S** | **I** | **Time** | **D** | **LongD** | **S** | **I** |
| 1980–2009 | 15 | 2.8 | 9 | 1.10 | 0.25 | | | | | |
| 2010–2039 | 16 | 3.5 | 10 | 1.53 | 0.31 | 14 | 3.21 | 9 | 1.33 | 0.278 |
| 2040–2069 | 20 | 3.6 | 19 | 1.55 | 0.36 | 25 | 3.2 | 17 | 1.37 | 0.249 |
| 2070–2100 | 22 | 3.7 | 18 | 1.80 | 0.36 | 22 | 3.37 | 17 | 1.79 | 0.401 |

*Note:* D, S, and I are average duration, severity, and intensity, whereas LongD is the longest duration.

century due to climate change, which more likely affects sorghum production mainly under RCP4.5 climate scenario at the study area. Similarly, drought frequency, duration and intensity are affected by climate change in East and West Africa (Polong *et al.* 2019; Ogunrinde *et al.* 2022). These prolonged dry spells, drought, rainfall variability and temperature increases are the most predominant stresses and have a significant influence on crop yield reduction (Srivastava *et al.* 2010).

**Table 4** | Drought characteristics in SPEI-4 based on ensemble mean across three GCMs

| | Under RCP4.5 climate forcing | | | | | Under RCP8.5 climate forcing | | | | |
|---|---|---|---|---|---|---|---|---|---|---|
| **Period** | **Time** | **D** | **LongD** | **S** | **I** | **Time** | **D** | **LongD** | **S** | **I** |
| 1980–2009 | 13 | 3.85 | 11 | 1.51 | 0.25 | | | | | |
| 2010–2039 | 13 | 4.54 | 18 | 2.1 | 0.31 | 12 | 4.17 | 17 | 1.79 | 0.262 |
| 2040–2069 | 14 | 4.71 | 19 | 2.38 | 0.36 | 18 | 4.0 | 19 | 2.05 | 0.343 |
| 2070–2100 | 18 | 4.33 | 19 | 2.29 | 0.38 | 18 | 4.1 | 18 | 2.19 | 0.374 |

*Note:* D, S, and I are average duration, severity, and intensity, whereas LongD is the longest duration in months.

**Table 5** | Drought characteristics in SPEI-6 based on ensemble mean across the GCMs

| | Under RCP4.5 climate forcing | | | | | Under RCP8.5 climate forcing | | | | |
|---|---|---|---|---|---|---|---|---|---|---|
| **Period** | **Time** | **D** | **LongD** | **S** | **I** | **Time** | **D** | **LongD** | **S** | **I** |
| 1980–2009 | 11 | 4.64 | 20 | 2.15 | 0.29 | | | | | |
| 2010–2039 | 11 | 5.64 | 25 | 2.77 | 0.30 | 10 | 5.0 | 20 | 2.47 | 0.308 |
| 2040–2069 | 10 | 6.2 | 25 | 3.44 | 0.40 | 12 | 6.7 | 25 | 3.19 | 0.35 |
| 2070–2100 | 14 | 5.0 | 20 | 2.91 | 0.39 | 14 | 4.8 | 20 | 2.67 | 0.332 |

*Note:* D, S, and I are average duration, severity, and intensity, whereas LongD is the longest duration in months.

### 3.5. Temporal drought frequency change in the SPI and SPEI

Changes in drought indices over the Babile district in 3-, 4- and 6-month time scales using SPI and SPEI drought indices presented in Figure 5(a) and Figure 5(b) during baseline period from 1980–2009, near-century (2010–2039), mid-century (2040–2069) and end (2070–2100) of the 21st century for indicating the worst period for proactive risk. The result revealed that based on ensemble mean across the three-model output showed SPI drought indices median change from –0.1 (2010–2039) to 0.15 (2040–2069) and 0.2 (2070–2100) month/year under RCP4.5 climate forcing (Figure 5(a)), while SPI median changes from 0.1 (2010–2039) to –0.2 (2040–2069) and 0.25 (2070–2100) month/year under RCP8.5 climate forcing (Figure 5(b)).

The SPEI drought indices indicated a moderate change in median values in the range −0.1 (2010–2039) month/year but no significant change in the mid and end of the 21st century under RCP4.5 climate forcing (Figure 6(a)). This result was

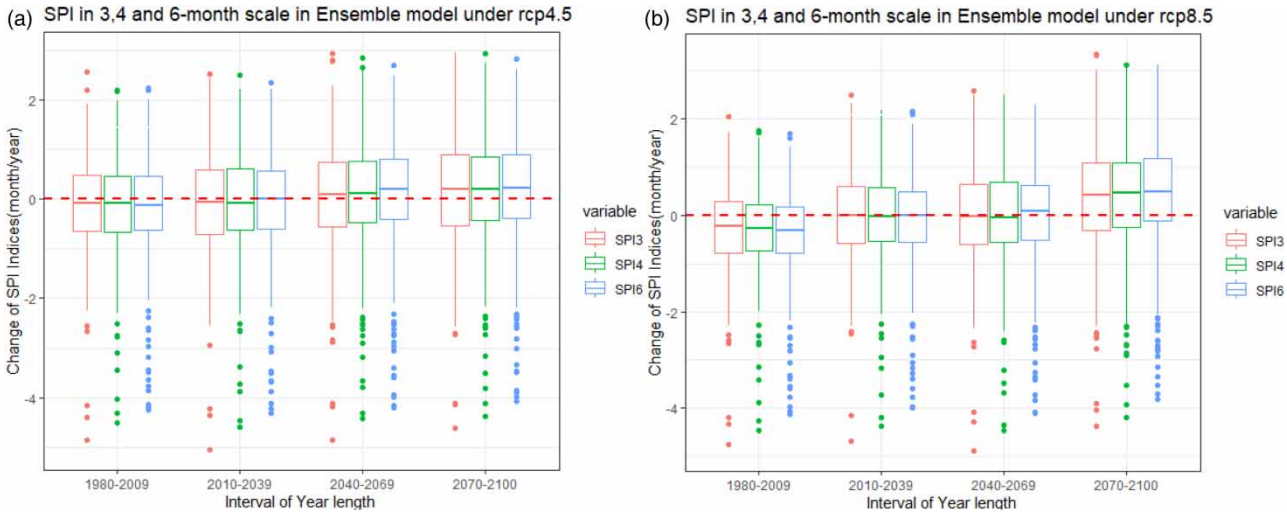


**Figure 5** | Changes in the SPI drought indices in the ensemble mean model under RCP4.5 and 8.5 scenarios.

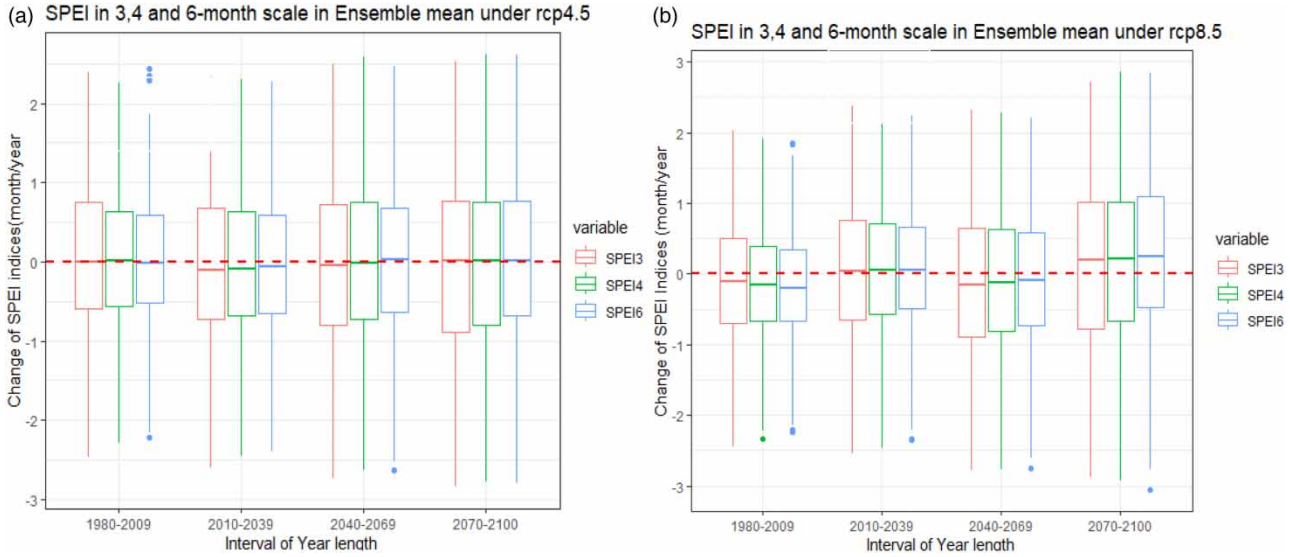


**Figure 6** | Changes in SPEI drought indices based on the ensemble mean value across GCM models.

substantially comparable with a previous study on global climate trend analysis, which stated 'the dry regions tend to get drier, and wet regions tend to get wetter' (Yang *et al.* 2019). Similarly, the study made by Haile *et al.* (2020) based on five GCMs climate models over East Africa stated that the magnitude of drought frequency occurrence in the arid and semi-arid parts of Ethiopia is likely to increase. On the other hand, the SPEI indices median changes 0.1 (2010–2039) to –0.2 (2040–2069) and 0.25 (2070–2100) month/year under RCP8.5 climate forcing (Figure 6(b)). Similarly, the previous study reported that consistent with the negative change in the magnitude and frequency of drought is higher (Oguntunde *et al.* 2018).

## 4. CONCLUSION

Evaluating drought characteristics in recent and future periods is vital for feasible adaptation strategies. The future rainfall and temperature trends were employed for the input for future drought characteristics analysis. The SPI and SPEI drought indices were used to assess the future impacts of climate change on drought duration severity and intensity under RCP4.5 and RCP8.5 future climate scenarios. The climate data of Babile meteorological station from 1980–2009 was used as a baseline for future climate projection using three global climate models, namely CanESM2, HadGEM2-ES and GGFDL-ESM2M used by the Intergovernmental Panel on Climate Change (IPCC) of the Fifth Assessment Report CMIP5) under two Representative Concentration Pathways (RCP4.5 and RCP8.5) for near, mid and end of the 21st century. The characteristics and trend of rainfall and temperature of the study area were analyzed. Drought characteristic indices of SPEI were evaluated based on temperature and rainfall while the SPI was based on rainfall. Drought characteristics such as duration, severity and intensity, which is the longest drought, the strongest severity of drought and the highest intensity of drought in the study area, have been identified within SPEI 3-, SPEI 4-, and SPEI 6-month scales related to agricultural crop production at the Babile District east Hararghe zone under RCP4.5 and RCP8.5 climate scenarios.

The results revealed that the annual maximum temperature would increase by 0.31 °C every 10 years and the annual minimum temperature increased by 0.22 °C every 10 years under the RCP4.5 scenario, whereas the annual maximum and minimum temperature increases by 0.48 and 0.46 °C in every 10 years under the RCP8.5 scenario. However, the rainfall trend varies with months and season's time scale. Consequently, the drought intensity and severity increase toward 21st century mainly under RCP4.5 in observed and mean across the three GCM climate model's output. The average drought durations (*D*) were 2.8, 3.5, 3.6 and 3.7 months in SPEI-3-month and 3.85, 4.54, 4.71 and 4.33 months in SPEI-4-month and 4.64, 5.64, 6.2 and 5 months in SPEI-6-month under RCP4.5 during observed, near, mid and end of 21st century respectively. Similarly, the average drought durations (*D*) were 3.21, 3.2 and 3.37 months in SPEI-3-month 4.17, 4 and 4.1 months in SPEI-4-month and 5, 6.7 and 4.8 months in SPEI-6-month under RCP8.5 during near, mid and end of 21st century. Increase in drought intensity and severity will affect sorghum production in in the future mainly under RCP4.5 scenarios. To tackle the

impacts of drought, soil water conservation practices and drought resistance variety and soil water conservation cropping system are highly recommended to adapt crop production under future climate scenarios over the study area.

## ACKNOWLEDGEMENTS

The authors would like to acknowledge the Ethiopia Meteorological Institute in the acquisition of necessary data and technical support for this work, who provided us climate data from 1980–2009 which was used as a baseline for future projection. We are also grateful to the African Center of Excellence in Climate Smart Agriculture and Biodiversity Conservation of Haramaya University for hosting a PhD study to undertake this research working facility and management support. The Authors also forward great thanks to those friends who stand by our side during the research work, share information as well as extended their technical support during the needed period. Momentous thank also goes to all anonymous reviewers for their valuable comments and remarks during the review process for further improvement of the manuscript.

## AUTHOR CONTRIBUTIONS

A.A.T. was responsible for all activities of the research process such as the design, data collection from all sources, data compilation, and entry, data analysis, interpretation of results, editing as well as writing up of the manuscript. The four authors D.K.D., L.W.M., Z.B.E., and F.M.L. were involved in supervising from design to data collection, contributed to framing the manuscript, made valuable inputs, edited, and commented on improving the quality of the manuscript during the write-up of the manuscript. All authors contributed to the manuscript, and read and approved the final submitted version.

## FUNDING

This research did not receive any specific grant from funding agencies in the public, commercial, or non-profit sectors.

## DATA AVAILABILITY STATEMENT

All relevant data are included in the paper or its Supplementary Information.

## CONFLICT OF INTEREST

The authors declare there is no conflict.

## REFERENCES

Abtew, W. & Melesse, A. 2013 Climate change and evapotranspiration. In: *Evaporation and Evapotranspiration: Measurements and Estimations*. Springer, Dordrecht, pp. 197–202.

Adhyani, N. L., June, T. & Sopaheluwakan, A. 2017 Exposure to drought: Duration, severity and intensity (Java, Bali and Nusa Tenggara). In: *IOP Conference Series: Earth and Environmental Science*, Vol. 58 (1). IOP Publishing, Bristol, UK, p. 012040.

Ahmed, K., Shahid, S. & Nawaz, N. 2018 Impacts of climate variability and change on seasonal drought characteristics of Pakistan. *Atmospheric Research* **214**, 364–374.

Allen, R. G., Pereira, L. S., Raes, D. & Smith, M. 1998 *Crop Evapotranspiration-Guidelines for Computing Crop Water Requirements*, Vol. 300 (9). FAO Irrigation and drainage paper 56. FAO, Rome, p. D05109.

Chylek, P., Li, J., Dubey, M. K., Wang, M. & Lesins, G. J. A. C. 2011 Observed and model simulated 20th century Arctic temperature variability: Canadian earth system model CanESM2. *Atmospheric Chemistry and Physics Discussions* **11** (8), 22893–22907.

Droogers, P. & Allen, R. G. 2002 Estimating reference evapotranspiration under inaccurate data conditions. *Irrigation and Drainage Systems* **16**, 33–45.

Dunne, J. P., John, J. G., Shevliakova, E., Stouffer, R. J., Krasting, J. P., Malyshev, S. L., Milly, P. C. D., Sentman, L. T., Adcroft, A. J., Cooke, W. & Dunne, K. A. 2013 GFDL's ESM2 global coupled climate–carbon earth system models. Part II: Carbon system formulation and baseline simulation characteristics. *Journal of Climate* **26** (7), 2247–2267.

Ejeta, G. & Knoll, J. E. 2007 Marker-assisted selection in sorghum. In: *Genomics-assisted Crop Improvement: Vol 2: Genomics Applications in Crops* (Varshney, R. K. & Tuberosa, R., eds). Springer Netherlands, Dordrecht, pp. 187–205.

Ekstrom, M., Grose, M. R. & Whetton, P. H. 2015 An appraisal of downscaling methods used in climate change research. *Wiley Interdisciplinary Reviews: Climate Change* **6** (3), 301–319.

Endris, H. S., Omondi, P., Jain, S., Lennard, C., Hewitson, B., Chang'a, L., Awange, J. L., Dosio, A., Ketiem, P., Nikulin, G. & Panitz, H. J. 2013 Assessment of the performance of CORDEX regional climate models in simulating East African rainfall. *Journal of Climate* **26** (21), 8453–8475.

Eslamian, S., Dalezios, N. R., Singh, V. P., Adamowski, J., Mohammadifard, S., Bahmani, R., Eskandari, S., Zomorodian, M., Arefeyan, A., Dehghani, S. & Aghaesmaeili, M. 2017 Drought management: Current challenges and future outlook. In: *Handbook of Drought and Water Scarcity* (Eslamian, S. & Eslamian, F. A., eds). CRC Press, Boca Raton, FL, USA, pp. 729–763.

FAO 2010 *Analysis of Climate Change and Variability Risks in the Smallholder Sector*. Department of Resource Surveys and Remote Sensing (DRSRS) in collaboration with the Food and Agriculture Organization of the United Nations, Rome.

Gong, L., Tian, B., Li, Y. & Wu, S. 2021 Phenological changes of soybean in response to climate conditions in frigid region in China over the past decades. *International Journal of Plant Production* **15**, 363–375.

Grillakis, M. G. 2019 Increase in severe and extreme soil moisture droughts for Europe under climate change. *Science of the Total Environment* **660**, 1245–1255.

Haile, G. G., Tang, Q., Hosseini-Moghari, S. M., Liu, X., Gebremicael, T. G., Leng, G., Kebede, A., Xu, X. & Yun, X. 2020 Projected impacts of climate change on drought patterns over East Africa. *Earth's Future* **8** (7), e2020EF001502.

Hargreaves, G. H. & Samani, Z. A. 1985 Reference crop evapotranspiration from temperature. *Applied Engineering in Agriculture* **1** (2), 96–99.

Hosking, J. R. 1990 L-moments: Analysis and estimation of distributions using linear combinations of order statistics. *Journal of the Royal Statistical Society Series B: Statistical Methodology* **52** (1), 105–124.

Martin, G. M. & Bellouin, N. 2011 HadGEM2 family of met office unified model climate configurations. *Geoscientific Model Development* **4**, 723–757.

McKee, T. B., Doesken, N. J. & Kleist, J. 1993 The relationship of drought frequency and duration to time scales. In *Proceedings of the 8th Conference on Applied Climatology*, Vol. 17 (22), pp. 179–183.

Meresa, H. K., Osuch, M. & Romanowicz, R. 2016 Hydro-meteorological drought projections into the 21-st century for selected Polish catchments. *Water* **8** (5), 206.

Mishra, A. K. & Singh, V. P. 2010 A review of drought concepts. *Journal of Hydrology* **391** (1–2), 202–216.

MoA (Ministry of Agriculture) 1998 Agro-ecological zones of Ethiopia. Natural Resources Management and Regulatory Department. With support of German Agency for Technical Cooperation (GTZ).

NMSA 1996 Climate and agro-climatic resources of Ethiopia, Meteorological Research Report Series. National Meteorological Services Agency, Vol.1, No.1, Addis Ababa. pp 137.

Ogilvie, A., Mahe, G., Ward, J., Serpantie, G., Lemoalle, J., Morand, P., Barbier, B., Diop, A. T., Caron, A., Namarra, R. & Kaczan, D. 2013 Water, agriculture and poverty in the Niger River basin. In: *Water, Food and Poverty in River Basins* (Fisher, M. & Cook, S., eds). Routledge, London, pp. 131–159.

Oguntunde, P. G., Lischeid, G. & Abiodun, B. J. 2018 Impacts of climate variability and change on drought characteristics in the Niger River Basin, West Africa. *Stochastic Environmental Research and Risk Assessment* **32**, 1017–1034.

Ogunrinde, A. T., Oguntunde, P. G., Akinwumiju, A. S., Fasinmirin, J. T., Olasehinde, D. A., Pham, Q. B., Linh, N. T. T. & Anh, D. T. 2022 Impact of climate change and drought attributes in Nigeria. *Atmosphere* **13** (11), 1874.

Omer, A., Zhuguo, M., Zheng, Z. & Saleem, F. 2020 Natural and anthropogenic influences on the recent droughts in Yellow River Basin, China. *Science of the Total Environment* **704**, 135428.

Pohlert, T. 2016 Non-parametric trend tests and change-point detection. *Creative Commons License (CC BY-ND)* **4**, 1–18.

Polong, F., Chen, H., Sun, S. & Ongoma, V. 2019 Temporal and spatial evolution of the standard precipitation evapotranspiration index (SPEI) in the Tana River Basin, Kenya. *Theoretical and Applied Climatology* **138**, 777–792.

Singh, P., Boote, K. J., Kadiyala, M. D. M., Nedumaran, S., Gupta, S. K., Srinivas, K. & Bantilan, M. C. S. 2017 An assessment of yield gains under climate change due to genetic modification of pearl millet. *Science of the Total Environment* **601**, 1226–1237.

Srivastava, A., Kumar, S. N. & Aggarwal, P. K. 2010 Assessment on vulnerability of sorghum to climate change in India. *Agriculture, Ecosystems & Environment* **138** (3–4), 160–169.

Sunyer, M. A., Madsen, H. & Ang, P. H. 2012 A comparison of different regional climate models and statistical downscaling methods for extreme rainfall estimation under climate change. *Atmospheric Research* **103**, 119–128.

Taylor, K. E., Stouffer, R. J. & Meehl, G. A. 2012 An overview of CMIP5 and the experiment design. *Bulletin of the American Meteorological Society* **93** (4), 485–498.

Teshome, A. & Zhang, J. 2019 Increase of extreme drought over Ethiopia under climate warming. *Advances in Meteorology* **2019**, 1–18.

Thom, H. C. S. 1966 *Some Methods of Climatological Analysis*, Vol. 81. Secretariat of the World Meteorological Organization, Geneva, p. 53.

Tolosa, A. A., Dadi, D. K., Mirkena, L. W., Erena, Z. B. & Liban, F. M. 2023 Impacts of climate variability and change on sorghum crop yield in the babile district of eastern Ethiopia. *Climate* **11** (5), 99.

Van Loon, A. F. 2015 Hydrological drought explained. *Wiley Interdisciplinary Reviews: Water* **2** (4), 359–392.

Vicente-Serrano, S. M., Beguería, S. & López-Moreno, J. I. 2010 A multiscale drought index sensitive to global warming: the standardized precipitation evapotranspiration index. *Journal of Climate* **23** (7), 1696–1718.

Wallach, D., Mearns, L. O., Ruane, A. C., Rötter, R. P. & Asseng, S. 2016 Lessons from climate modeling on the design and use of ensembles for crop modeling. *Climatic Change* **139**, 551–564.

Wang, Y., Liu, G. & Guo, E. 2019 Spatial distribution and temporal variation of drought in Inner Mongolia during 1901–2014 using standardized precipitation evapotranspiration index. *Science of the Total Environment* **654**, 850–862.

Yang, T., Ding, J., Liu, D., Wang, X. & Wang, T. 2019 Combined use of multiple drought indices for global assessment of dry gets drier and wet gets wetter paradigm. *Journal of Climate* **32** (3), 737–748.

Zelen, M., Severo, N. C., 1965 Probability functions. In: *Handbook of Mathematical Functions with Formulas, Graphs, and Mathematical Tables* (Abramowitz, M. & Stegun, I. A., eds.). National Bureau of Standards Applied Mathematics Series-55, US Government Printing Office, Washington, DC.

Zhou, Q., Yang, S., Zhao, C., Cai, M., Lou, H., Luo, Y. & Hou, L. 2016 Development and implementation of a spatial unit non-overlapping water stress index for water scarcity evaluation with a moderate spatial resolution. *Ecological Indicators* **69**, 422–433.

First received 18 December 2023; accepted in revised form 8 July 2024. Available online 23 July 2024